contributes to the overlapping of the $Cu^{II}Cu^{II}/Cu^{II}Cu^{I}$ and $Cu^{II}Cu^{I}/Cu^{I}Cu^{I}$ redox steps.

Comparisons of the EPR spectra in solution and in the solid state, Figure 5, afford further evidence for localized oxidation states within the dinuclear unit. The powder spectrum (Figure 5a) consists of one broad, nearly isotropic signal (ΔH_{tot} = 225 (2) G) centered at g_{av} = 2.079 (3). The second derivative temperature-dependent line shape does not give evidence to any change in spectral shape, with no appearance of hyperfine splitting. This strongly indicates the presence of remarkable magnetic coupling between the Cu(II) centers in the tetrameric unit.[43] In contrast, as expected for one unpaired electron residing on the Cu(2) atom,[36-40,44] the glassy spectrum reveals a well-resolved axial structure ($g_{\parallel} > g_{\perp}$) with the hyperfine parallel components centered at $g_{\parallel}$ = 2.342 (3) with $A_{\parallel}$ = 133 (3) G. The unresolved perpendicular absorption exhibits a relatively sharp line ($\Delta H_{\perp}$ = 70 (2) G) at $g_{\perp}$ = 2.088 (3). A g_{iso} value of 2.173 (3) can be thus computed. At room temperature the spectrum exhibits a poorly resolved line shape (ΔH_{iso} = 140 (2) G) centered at g_{iso} = 2.165 (5).

Figure 6 gives the X-band EPR spectra recorded both at liquid-nitrogen and ambient temperature on a DMSO solution of $Cu_2(memi)Br_3$ after exhaustive one-electron anodic oxidation to the corresponding $Cu^{II}Cu^{II}$ congener. The glassy spectrum is indicative of the presence of two copper(II) centers, magnetically noninteracting. It is characteristic of axial structures ($g_{\perp_{1,2}} < g_{\parallel_{1,2}}$). The line shape of the parallel region provides evidence for a "four plus four" hyperfine pattern attributable to two distinct cupric centers. The spectroscopic parameters indicate the presence of the untouched Cu(2) center ($g_{\parallel}$ = 2.346 (3), $g_{\perp}$ = 2.088 (3), $A_{\parallel}$ = 132 (3) G) together with the hyperfine parallel absorptions of the now oxidized Cu(1) center ($g_{\parallel}$ = 2.400 (3), $g_{\perp} \approx$ 2.097 (3), $A_{\parallel}$ = 116 (3) G). The calculated g_{iso} value is 2.198 (3), with a broadening of the perpendicular absorption ($\Delta H_{\perp}$ = 90 (3) G) with respect to the one of the mixed-valent precursor. The room-temperature spectrum is not resolved, but the increase in the overall linewidth (ΔH_{iso} = 185 (2) G; g_{av} = 2.160 (5)), together with the shift of the $g_{\perp}$ value in the glassy state agree with the interpretation of the spectrum as the sum of two distinct contributions from two noninteracting cupric species.

Finally, the apparent quasi-reversibility of the $Cu^{II}Cu^{II}/Cu^{II}Cu^{I}/Cu^{I}Cu^{I}$ electrochemical sequence must be considered. Departure from electrochemical reversibility may be taken as a probe for the occurrence of significant molecular reorganizations upon electron transfers.[45] However, in the case of dinuclear species, the peak-to-peak separation ΔE_p has to be related not only to the extent of electrochemical reversibility, but also to the extent of overlapping of the two one-electron transfers. On the bases of the actual data, it is hardly appropriate to speculate on the stereochemical reorganizations that will accompany oxidation to $Cu^{II}Cu^{II}$ or reduction to $Cu^{I}Cu^{I}$. Attempts to grow crystals of such congeners in order to evaluate the precise structural rearrangement accompanying these redox changes have not been successful as yet.

Acknowledgment. We gratefully acknowledge the technical assistance from ISSECC, CNR, Florence, Italy, in making susceptibility and conductivity measurements.

Registry No. $[Cu_2(memi)Br_3]_x$, 129493-04-5.

Supplementary Material Available: Tables of hydrogen atom coordinates and anisotropic thermal parameters of non-hydrogen atoms for $Cu_2(C_7H_{12}N_2S)Br_3$ (2 pages); a table of structure factors for $Cu_2(C_7H_{12}N_2S)Br_3$ (11 pages). Ordering information is given on any current masthead page.

(43) Hathaway, B. J. *Struct. Bonding* **1984**, *57*, 55.
(44) Mandal, S. K.; Thompson, L. K.; Nag, K. *Inorg. Chim. Acta* **1988**, *149*, 247.
(45) Zanello, P. *Stereochemistry of Organometallic and Inorganic Compounds*; Bernal, I., Ed.; Elsevier: Amsterdam, in press; Vol. 4, and references therein.

Contribution from the Departments of Chemistry, Abilene Christian University, Abilene, Texas 79699, and University of Missouri—Rolla, Rolla, Missouri 65401

Infrared, Magnetic, Mössbauer, and Structural Characterization of $Fe(TPP)(OReO_3)\cdot tol$ (TPP = Dianion of Tetraphenylporphyrin; tol = Toluene)

LaNelle Ohlhausen, David Cockrum, Jay Register, Kent Roberts, Gary J. Long,† Gregory L. Powell,*,‡ and Bennett B. Hutchinson*,§

Received September 14, 1989

Perrhenatoiron(III) tetraphenylporphyrin has been isolated as its toluene solvate and characterized by using magnetic susceptibility, IR and Mössbauer spectroscopy, and single-crystal X-ray diffraction. Crystal data at 20 °C are a = 12.228 (3) Å, b = 12.235 (3) Å, c = 15.968 (4) Å, α = 88.35 (2)°, β = 103.67 (2)°, γ = 113.18 (2)°, Z = 2, and space group $P\bar{1}$. The iron atom is shown to be pentacoordinate with the perrhenate ion bound in a monodentate arrangement. The average Fe–N distance is 2.059 (7) Å, and the Fe–O bond distance is 2.024 (9) Å. The toluene molecules are present at a 43° angle to the porphyrin plane. No π-bonding between the solvent and porphyrin or between porphyrin moieties is evident. Two Re–O stretching and bending vibrations at 942, 827 cm^{-1} and at 336, 321 cm^{-1}, respectively, also support the monodentate coordination of the perrhenate. The compound has a magnetic moment of 5.5 μ_B at 298 K arising from a quantum-mechanical admixture of $S = {}^5/_2$ and $S = {}^3/_2$ iron spin states in which the ${}^5/_2$ state predominates. The 78 K Mössbauer spectrum shows a quadrupole doublet with parameters consistent with this admixture, and the spectral line shape may indicate the presence of electronic relaxation between the two states on the Mössbauer time scale.

Introduction

Over the past decade, paralleling the rise in interest in metalloporphyrin chemistry, several iron(III) porphyrin compounds possessing oxyanionic ligands in the axial position have been characterized. A primary motivation for this work arose because hemoporphyrins with oxygenated ligands provide a framework for understanding important biological systems containing Fe–O bonds, and much novel coordination chemistry has been realized as well.

Solid-state structural characterization of iron(III) porphyrins with the oxyanions ClO_4^-, NO_3^-, $CH_3CO_2^-$, OR^-, SO_4^{2-}, $OTeF_5^-$, and OSO_3H^- has provided examples of monodentate, simple bidentate, and bridging bidentate coordination of the oxyanion.[1-10]

* To whom correspondence should be addressed.
† University of Missouri—Rolla.
‡ Address correspondence to this author at Abilene Christian University.
§ Address correspondence to this author at Department of Chemistry, Pepperdine University, Malibu, CA 90263.

(1) Reed, C. R.; Mashiko, T.; Bentley, S. P.; Kastner, M. E.; Scheidt, W. R.; Spartalian, D.; Lang, G. *J. Am. Chem. Soc.* **1979**, *101*, 2948.

0020-1669/90/1329-4886$02.50/0

Table I. Crystallographic Data for Fe(TPP)($OReO_3$)·C_7H_8

chem formula $ReFeO_4N_4C_{51}H_{36}$	fw 1010.9
a = 12.228 (3) Å	space group $P\bar{1}$
b = 12.235 (3) Å	T = 20 ± 1 °C
c = 15.968 (4) Å	λ = 0.71073 Å
α = 88.35 (2)°	ρ_{calcd} = 1.577 g/cm^3
β = 103.67 (2)°	μ = 32.70 cm^{-1}
γ = 113.18 (2)°	$R(F_o)$ = 0.0595
V = 2128 (1) Å^3	$R_w(F_o^2)$ = 0.0811
Z = 2	transm coeff = 0.757–1.000

In addition to this variety of coordination modes, some Fe(porphyrin)X, where X is an oxyanion, compounds have shown pure high-spin, $S = {}^5/_2$, states while others have admixed quantum $S = {}^3/_2$ and ${}^5/_2$ iron(III) spin states.[1-10] Of particular interest has been Fe^{III}(TPP)($OClO_3$), which exhibits an intermediate-spin state that has been accounted for by using quantum admixed spin states and which serves as a model compound of the naturally occurring ferricytochrome c'.[1,2,11] Consequently, it was of interest to examine the effect of the ReO_4^- ligand, which possesses a geometry similar to that of ClO_4^- but a slightly better coordinating ability, on the stereochemistry and iron spin state. Fe(TPP)(ReO_4) has been prepared previously in solution, and its pyrrole proton chemical shift values have been measured.[12]

Our goal has been to characterize Fe(TPP)(ReO_4) by utilizing IR spectroscopy, magnetic susceptibility, X-ray diffraction, and Mössbauer spectral techniques to determine its spin state, coordination number, molecular structure, and packing arrangement and to compare those findings with the properties of its congeners.

Two reviews by Scheidt provide background for this work: one[13] on the control of spin states in these systems and the other[14] organizing and discussing the stereochemistry of metallotetrapyrroles.

Experimental Section

Materials. Reactions were carried out in freshly distilled solvents, which were degassed before use. Fe(TPP)Cl was obtained from Strem Chemicals, Inc., Newburyport, MA. Other chemicals used were of reagent grade.

Preparation of Fe(TPP)($OReO_3$). $AgReO_4$ was refluxed with Fe(TPP)Cl in benzene for 3 h, the solution filtered, and the benzene removed at room temperature. The resulting purple compound was dissolved in 15 mL of chloroform, the solution filtered, and the chloroform removed at room temperature. The resulting blue-brown precipitate was washed in hexane and dried overnight in vacuo at 50 °C. An 87.0% yield was obtained for the nonsolvated Fe(TPP)($OReO_3$) based on Fe(TPP)Cl. Anal. Calcd for $C_{44}H_{28}N_4O_4FeRe$: C, 57.52; H, 3.07; N, 6.10. Found: C, 57.67; H, 3.13; N, 6.04.

Preparation of Fe(TPP)($OReO_3$)·tol. Fe(TPP)($OReO_3$) was recrystallized from toluene and the product dried in vacuo at 50 °C overnight. Anal. Calcd for $C_{51}H_{36}N_4O_4FeRe$: C, 60.59; H, 3.59; N, 5.54. Found: C, 60.47; H, 3.63; N, 5.54.

Crystal Structure. Dark purple crystals were obtained by slow evaporation of a CH_2Cl_2/toluene solution. A crystal of dimensions 0.32 × 0.50 × 0.65 mm was glued with epoxy cement to the inside of a sealed, thin-walled glass capillary. X-ray data collection (Mo Kα radiation), an empirical absorption correction based on six ψ scans, and Lorentz and polarization corrections were carried out at Crystalytics Co., Lincoln, NE. All subsequent calculations were done on a VAX-11/785 computer at ACU with use of the SDP-VAX and SHELX-76 software packages. Data collection and refinement parameters are summarized in Table I.

The structure was solved by analysis of a Patterson map. All nonhydrogen atoms were located and isotropically refined with use of the SDP-VAX software. During the final stages of full-matrix least-squares refinement, it became obvious that the toluene molecule was slightly disordered with a secondary methyl group at low occupancy. All at-

Table II. Atomic Positional and Isotropic Equivalent Thermal Parameters for Fe(TPP)($OReO_3$)·C_7H_8

atom	x	y	z	V, Å^2[a]
Re	0.35565 (5)	0.02541 (5)	0.19165 (4)	4.32 (2)
Fe	0.3315 (1)	0.2733 (1)	0.26327 (8)	2.13 (4)
O(1)	0.3982 (6)	0.1758 (6)	0.2062 (4)	2.9 (2)
O(2)	0.2135 (9)	−0.0490 (9)	0.1274 (7)	7.5 (4)
O(3)	0.459 (1)	0.011 (1)	0.1437 (8)	7.3 (4)
O(4)	0.364 (1)	−0.0339 (9)	0.2894 (7)	6.6 (4)
N(1)	0.4437 (7)	0.4459 (6)	0.2511 (5)	2.6 (2)
N(2)	0.4318 (7)	0.2923 (7)	0.3893 (5)	2.6 (2)
N(3)	0.1907 (7)	0.1390 (7)	0.3019 (5)	2.3 (2)
N(4)	0.2002 (7)	0.2957 (7)	0.1650 (5)	2.3 (2)
C(A1)	0.431 (1)	0.5128 (8)	0.1791 (6)	3.0 (3)
C(A2)	0.541 (1)	0.6164 (9)	0.1869 (8)	3.8 (3)
C(A3)	0.622 (1)	0.6167 (9)	0.2623 (7)	3.7 (3)
C(A4)	0.5596 (9)	0.5078 (8)	0.3021 (7)	2.9 (3)
C(A5)	0.6106 (9)	0.4757 (9)	0.3808 (7)	3.0 (3)
C(A6)	0.7431 (9)	0.5552 (9)	0.4241 (7)	3.1 (3)
C(A7)	0.770 (1)	0.639 (1)	0.489 (1)	5.3 (4)
C(A8)	0.888 (1)	0.708 (1)	0.528 (1)	6.0 (5)
C(A9)	0.982 (1)	0.700 (1)	0.5052 (9)	5.5 (4)
C(A10)	0.960 (1)	0.616 (2)	0.439 (1)	7.0 (6)
C(A11)	0.835 (1)	0.542 (1)	0.3974 (9)	5.7 (5)
C(B1)	0.550 (1)	0.3789 (9)	0.4218 (6)	3.0 (3)
C(B2)	0.602 (1)	0.351 (1)	0.5057 (7)	4.3 (4)
C(B3)	0.510 (1)	0.247 (1)	0.5251 (7)	4.2 (3)
C(B4)	0.4089 (9)	0.2126 (9)	0.4508 (6)	3.0 (3)
C(B5)	0.3024 (9)	0.1118 (9)	0.4452 (6)	2.8 (3)
C(B6)	0.2965 (9)	0.033 (1)	0.5203 (7)	3.2 (3)
C(B7)	0.248 (2)	0.053 (2)	0.585 (1)	8.4 (8)
C(B8)	0.250 (2)	−0.018 (2)	0.659 (1)	10 (1)
C(B9)	0.295 (1)	−0.104 (9)	0.6641 (9)	5.5 (5)
C(B10)	0.335 (1)	−0.123 (1)	0.599 (1)	5.9 (5)
C(B11)	0.337 (1)	−0.055 (1)	0.5250 (8)	4.8 (4)
C(C1)	0.2019 (9)	0.0769 (9)	0.3752 (6)	2.6 (3)
C(C2)	0.091 (1)	−0.027 (1)	0.3686 (7)	3.4 (3)
C(C3)	0.012 (1)	−0.0316 (9)	0.2904 (7)	3.3 (3)
C(C4)	0.0766 (9)	0.0748 (8)	0.2500 (6)	2.6 (3)
C(C5)	0.0255 (8)	0.1054 (8)	0.1703 (6)	2.6 (3)
C(C6)	−0.1010 (8)	0.0211 (8)	0.1227 (6)	2.6 (3)
C(C7)	−0.2042 (9)	0.0411 (9)	0.1285 (6)	2.9 (3)
C(C8)	−0.3209 (9)	−0.044 (1)	0.0836 (8)	4.2 (4)
C(C9)	−0.332 (1)	−0.143 (1)	0.0363 (8)	3.9 (3)
C(C10)	−0.230 (1)	−0.159 (1)	0.0300 (9)	5.0 (4)
C(C11)	−0.113 (1)	−0.078 (1)	0.0751 (8)	4.6 (4)
C(D1)	0.0819 (9)	0.2099 (8)	0.1326 (6)	2.5 (3)
C(D2)	0.0229 (9)	0.2491 (9)	0.0537 (6)	3.0 (3)
C(D3)	0.1084 (9)	0.358 (1)	0.0408 (7)	3.2 (3)
C(D4)	0.2184 (9)	0.3850 (8)	0.1095 (6)	2.7 (3)
C(D5)	0.3267 (9)	0.4851 (8)	0.1146 (6)	2.7 (3)
C(D6)	0.3312 (9)	0.5685 (9)	0.0415 (7)	2.9 (3)
C(D7)	0.306 (1)	0.668 (1)	0.0512 (8)	4.8 (4)
C(D8)	0.315 (1)	0.747 (1)	−0.015 (1)	5.7 (5)
C(D9)	0.347 (1)	0.728 (1)	−0.0866 (9)	4.4 (4)
C(D10)	0.371 (1)	0.628 (1)	−0.0972 (8)	4.7 (4)
C(D11)	0.362 (1)	0.545 (1)	−0.0301 (7)	4.3 (4)
C(S1)	0.009 (1)	0.618 (2)	0.213 (1)	10.4 (6)[b]
C(S2)	−0.030 (1)	0.495 (2)	0.222 (1)	9.1 (5)[b]
C(S3)	0.055 (1)	0.447 (2)	0.258 (1)	13.2 (8)[b]
C(S4)	0.179 (1)	0.521 (2)	0.284 (1)	9.6 (5)[b]
C(S5)	0.218 (1)	0.643 (2)	0.274 (1)	9.9 (6)[b]
C(S6)	0.133 (1)	0.692 (2)	0.239 (1)	12.1 (7)[b]
C(S7)	−0.077 (3)	0.673 (3)	0.194 (2)	18 (1)[b]

[a] Anisotropically refined atoms are given in the form of the isotropic equivalent displacement parameter defined as ${}^4/_3[a^2\beta_{11} + b^2\beta_{22} + c^2\beta_{33} + ab(\cos\gamma)\beta_{12} + ac(\cos\beta)\beta_{13} + bc(\cos\alpha)\beta_{23}]$. [b] Refined isotropically.

(2) Masuda, H.; Taga, T.; Osaki, K.; Sugimoto, H.; Yoshia, Z.; Ogoshi, H. *Inorg. Chem.* **1980**, *19*, 950.
(3) Phillippi, M. S.; Baenzinger, N.; Goff, H. M. *Inorg. Chem.* **1981**, *20*, 3904.
(4) Oumous, H.; Lecomte, C.; Protas, J.; Cocolios, P.; Guilard, R. *Polyhedron* **1984**, *3*, 651.
(5) Goff, H.; Shimomura, E. T.; Lere, Y. J.; Scheidt, W. R. *Inorg. Chem.* **1984**, *23*, 315.
(6) Stevens, E. D. *J. Am. Chem. Soc.* **1981**, *103*, 5087.
(7) Lecomte, C.; Chadwick, D. C.; Coppens, P.; Steven, E. D. *Inorg. Chem.* **1983**, *22*, 2982.
(8) Scheidt, W. R.; Lee, Y. J.; Bartzcak, T.; Hatano, K. *Inorg. Chem.* **1984**, *23*, 2552.
(9) Kellett, P. J.; Pawlid, M. J.; Taylor, L. R.; Thompson, R. G.; Levstik, M. A.; Anderson, O. P.; Strauss, S. H. *Inorg. Chem.* **1989**, *28*, 4400.
(10) Scheidt, W. R.; Lee, Y. J.; Finnegan, M. G. *Inorg. Chem.* **1988**, *27*, 4725.
(11) Maltempo, M. M. *J. Chem. Phys.* **1974**, *61*, 2540.
(12) Godziela, G. M.; Ridnour, L. A.; Goff, H. M. *Inorg. Chem.* **1985**, *24*, 1610.
(13) Scheidt, W. R.; Reed, C. A. *Chem. Rev.* **1981**, *81*, 543.
(14) Scheidt, W. R.; Lee, Y. J. *Struct. Bonding* **1987**, *64*, 1.

tempts to refine a disordered model led to unreasonable bond distances and angles. Refinement was concluded with use of the block-diagonal least-squares routine of SHELX-76, and the toluene molecule was refined as a rigid group. All non-hydrogen atoms except for those of the toluene molecule were refined anisotropically. No hydrogen atoms were included in the refinement. The final discrepancy indices were $R = 0.059$ and $R_w = 0.081$. The highest peak (1.234 e/Å^3) in a final difference Fourier map was the secondary methyl group of the toluene molecule as described above. The next two peaks (1.219 and 1.165 e/Å^3) were less than 0.6 Å away from the iron atom. A fourth peak (1.100 e/Å^3) was also close to the toluene molecule. There were no other peaks with heights above 0.9 e/Å^3. Final atomic coordinates and isotropic equivalent thermal parameters are given in Table II.

Magnetic Susceptibility. Magnetic susceptibility measurements were performed at 298 K on a Cahn/Ventron RM-2 electrobalance with $HgCo(SCN)_4$ as the susceptibility calibrant. The measurements were corrected for the diamagnetic susceptibilities ($\mu = 4.42 \times 10^{-6}$ cgsu) of the constituent atoms. Repeated measurements of several independently prepared samples gave a magnetic moment of 5.5 ± 0.1 μ_B at 298 K for Fe(TPP)($OReO_3$)·tol.

Spectroscopic Measurements. The IR spectra were measured as Nujol mulls on CsI plates with a PE-983 IR spectrophotometer. The UV–visible spectra were measured from 900 to 300 nm on 10^{-4} and 10^{-5} M solutions of Fe(TPP)($OReO_3$) in toluene by using a PE Lambda 5 UV–visible spectrophotometer [λ_{max} (nm), ϵ: 688 nm, 2×10^3; 571 nm, 2×10^3; 509 nm, 9×10^3; 415 nm, 8.8×10^3]. Nuclear magnetic resonance spectra were recorded in chloroform on a General Electric QE-300 FT-NMR spectrometer operating at 300.12 MHz at room temperature, referenced to TMS. The Mössbauer spectrum was measured at 78 K on a conventional constant-acceleration spectrometer that utilized a rhodium matrix cobalt-57 source and foil. The spectrum was fit by using conventional least-squares computer minimization techniques with one quadrupole doublet with Lorentzian line shape components of equal area but with different line widths.

Results and Discussion

Infrared Spectroscopy of Fe(TPP)($OReO_3$)·tol. IR spectroscopy has been successfully employed in characterizing oxyanion coordination modes.[15] For XY_4 anions one broad, strong absorption generally indicates that the anion serves an ionic function, whereas two sharper bands indicate C_{3v} symmetry and covalent monodentate coordination and three bands indicate C_{2v} symmetry and bidentate coordination. Previous studies place the ν_3 perrhenate stretching modes in the region around 920 cm^{-1}.[15,16] In addition to perrhenate stretching bands, this spectral region may contain absorptions due to TPP and toluene vibrations.

The IR spectrum of Fe(TPP)($OReO_3$)·tol was compared to the Fe(TPP)Cl spectrum[17] in the 700–1000-cm^{-1} region (see Figure 1) in order to locate the perrhenate bands. Two intense bands at 942 and 827 cm^{-1} are assigned as perrhenate stretching vibrations. Other bands appear in this region but are also present in the Fe(TPP)Cl spectrum and are assigned as modes due to TPP motions, with the exception of the 728-cm^{-1} band, which is assigned as a toluene absorption because it also appears as a strong band in the IR spectrum of toluene.[18] These perrhenate stretching assignments are supported by the IR spectra of $[Co(NH_3)_5(OH_2)]ReO_4 \cdot 2H_2O$ and $[Co(NH_3)_5(OReO_3)]Cl_2$, which illustrate ionic and monodentate perrhenate coordination, respectively.[16] The ionic perrhenate vibration occurs at 890 cm^{-1} in the cobalt hydrate but appears as two separate bands at 935 and 840 cm^{-1} in the compound with coordinated perrhenate.

In addition, two bands appear in the ν_4 ReO_4^- region[19,20] of Fe(TPP)($OReO_3$)·tol at 336 and 321 cm^{-1} but are not present in the IR spectrum of Fe(TPP)Cl. These are assigned as Re–O deformation bands. These IR spectral assignments clearly support monodentate coordination of the perrhenate in Fe(TPP)($OReO_3$)·tol, because the local C_{3v} symmetry of the Fe($OReO_3$) would provide two IR-active ReO_4 stretching and bending bands.

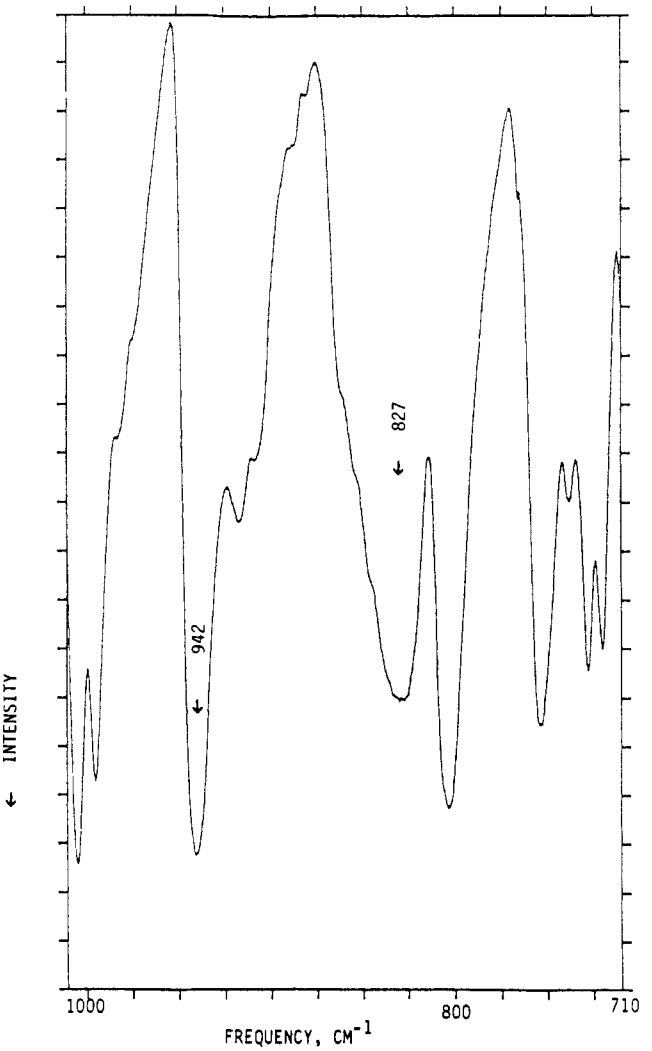

Figure 1. Infrared spectrum of Fe(TPP)($OReO_3$)·tol from 1010 to 710 cm^{-1}.

Table III. Selected Bond Distances and Angles for Fe(TPP)($OReO_3$)·C_7H_8

Distances (Å)			
Re–O(1)	1.711 (7)	Fe–N(1)	2.050 (7)
Re–O(2)	1.694 (9)	Fe–N(2)	2.061 (7)
Re–O(3)	1.69 (1)	Fe–N(3)	2.065 (7)
Re–O(4)	1.70 (1)	Fe–N(4)	2.060 (8)
Fe–O(1)	2.024 (9)		
Angles (deg)			
O(1)–Re–O(2)	114.7 (5)	O(1)–Fe–N(4)	104.5 (3)
O(1)–Re–O(3)	105.0 (4)	N(1)–Fe–N(2)	87.8 (3)
O(1)–Re–O(4)	109.4 (4)	N(1)–Fe–N(3)	156.0 (4)
O(2)–Re–O(3)	108.3 (6)	N(1)–Fe–N(4)	87.2 (3)
O(2)–Re–O(4)	109.0 (5)	N(2)–Fe–N(3)	86.6 (3)
O(3)–Re–O(4)	110.3 (6)	N(2)–Fe–N(4)	154.3 (4)
O(1)–Fe–N(1)	103.5 (3)	N(3)–Fe–N(4)	87.8 (3)
O(1)–Fe–N(2)	101.2 (3)	Re–O(1)–Fe	132.0 (4)
O(1)–Fe–N(3)	100.4 (3)		

Structural Features of Fe(TPP)($OReO_3$)·tol. Important bond distances and angles for Fe(TPP)($OReO_3$)·tol are given in Table III, and the molecular structure of the Fe(TPP)($OReO_3$) moiety is illustrated in Figure 2. The parameters of the iron coordination sphere include an Fe–O bond distance of 2.024 (9) Å, an average Fe–N bond distance of 2.059 (7) Å, and a displacement of the iron atom of 0.44 Å from the mean plane of the four nitrogen atoms. Clearly, the iron atom is pentacoordinate and the perrhenate ligand is monodentate. The overall geometry is similar to that of the metalloporphyrin molecule in Fe(TPP)($OClO_3$)·

(15) Nakamoto, K. *Infrared and Raman Spectra of Inorganic and Coordination Compounds*, 4th ed.; Wiley Interscience: New York, 1986.
(16) Lenz, E.; Murmann, R. K. *Inorg. Chem.* **1968**, *7*, 1882.
(17) Register, J.; Hutchinson, B. Unpublished results.
(18) Pouchert, C. J. *The Aldrich Library of FT-IR Spectra*, 1st ed.; Aldrich Chemical Co., Inc.: Milwaukee, WI, 1985; Vol. 2.
(19) Benciveni, L.; Nagarathna, H. M.; Gingerich, K. A. *Chem. Phys. Lett.* **1983**, *99*, 258.
(20) Varfolomeev, M. B.; Sharmarai, N. B.; Bardin, V. A.; Savel'eva, A. D.; Fomichev, V. V. *Russ. J. Inorg. Chem. (Engl. Transl.)* **1986**, *31*, 346.

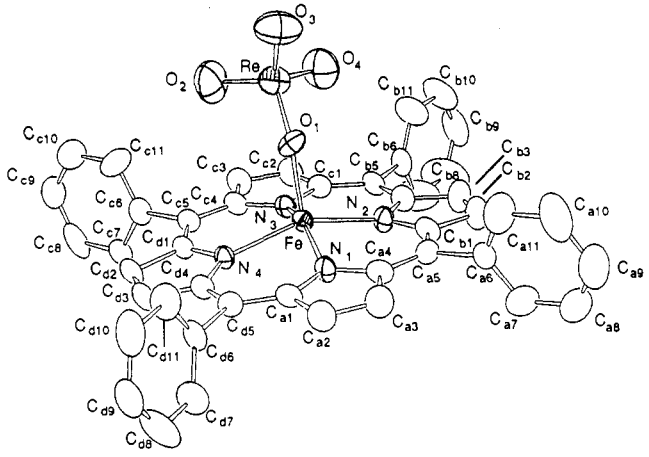

Figure 2. ORTEP view of the structure of the Fe(TPP)(OReO$_3$) molecule in Fe(TPP)(OReO$_3$)·tol. Ellipsoids are at the 50% probability level.

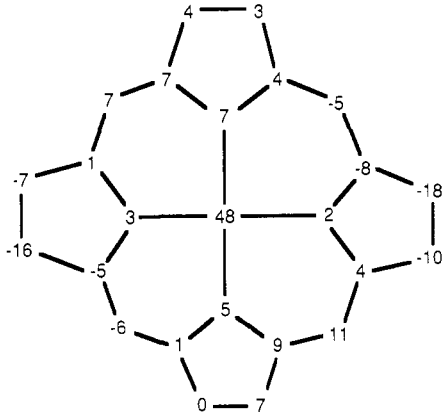

Figure 3. Illustration of the porphinato skeleton in Fe(TPP)(OReO$_3$)·tol showing the perpendicular displacements (in units of 0.01 Å) of each atom from the mean plane of the core.

0.5xyl[1] (xyl = *m*-xylene), but a variety of significant differences exist which are discussed below.

A diagram of the porphinato core that displays the perpendicular displacements of each atom from the mean plane appears in Figure 3. The core is almost planar, but is best described as a slightly folded "roof"[21] with approximate C_2 symmetry. In contrast, a ruffled conformation with approximate S_4 symmetry was observed in Fe(TPP)(OClO$_3$)·0.5xyl.[1] Maximum perpendicular displacements (excluding the iron atom) from the mean plane of the core are 0.18 and 0.29 Å for Fe(TPP)(OReO$_3$)·tol and Fe(TPP)(OClO$_3$)·0.5xyl, respectively. Not only is the porphyrin core more nearly planar in the perrhenate complex, but also the phenyl groups are more nearly perpendicular to the core; the average dihedral angle between the phenyl groups and the mean plane of the core is 84.0 (3)° for Fe(TPP)(OReO$_3$)·tol and 78.7 (2)° for Fe(TPP)(OClO$_3$)·0.5xyl. These observations suggest that there are significantly different crystal packing arrangements in these two species. In Fe(TPP)(OClO$_3$)·0.5xyl, the molecules pack in a porphyrin–solvate–porphyrin sandwich arrangement of essentially parallel rings, with an average distance of 3.5 (±0.15) Å between the *m*-xylene carbon atoms and the porphyrin plane and with $^1/_2$ mol of *m*-xylene/mol of porphyrin.[1] Figure 4 shows two views of the packing of Fe(TPP)(OReO$_3$) and toluene molecules in the crystal, which has 1 mol of toluene/mol of porphyrin. The Fe(TPP)(OReO$_3$) molecules pack in a stair-step-like arrangement. The angle between porphyrin and toluene planes is 43 (1)°.

Why should Fe(TPP)(OClO$_3$) and Fe(TPP)(OReO$_3$) have such different crystal packing arrangements, especially since the Fe–O–X angles are similar in each compound? An important consideration may be the fact that the perrhenate group is much larger than the perchlorate group. Interestingly, the unit cell volumes per non-hydrogen atom are essentially the same (17.4 Å^3 in the OReO$_3^-$ case and 17.3 Å^3 in the OClO$_3^-$ case) indicating that there is no significant difference in the "looseness" of the crystal packing. Perhaps the full mole of the solvent in Fe(TPP)(OReO$_3$)·tol just compensates for any additional space introduced by the larger oxyanion.

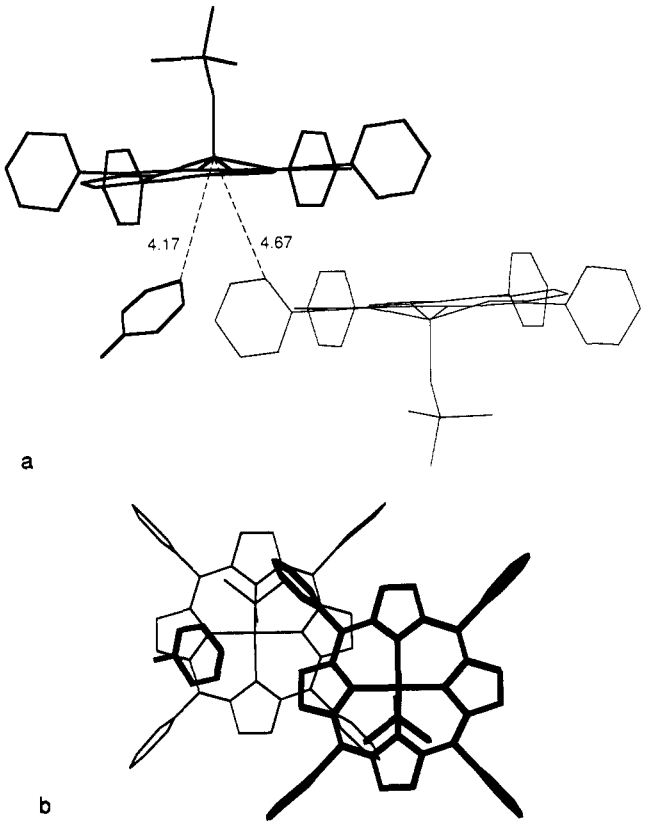

Figure 4. Two views of the positioning of Fe(TPP)(OReO$_3$) and toluene molecules in crystalline Fe(TPP)(OReO$_3$)·tol. Bolder lines are indicative of moieties that are closer to the viewer. (a) Top: view that is essentially perpendicular to the plane of the porphinato core. The closest distances from the iron atom to the toluene molecule and the TPP ligand are given in angstroms. (b) Bottom: view from another perspective (at a right angle to the first view and parallel with the porphinato core) that shows the small extent of overlap between porphyrin entities. The molecule represented with lighter lines in part a is in bolder lines in this figure, as if the viewer were looking up from the bottom of diagram a.

Also of interest is the apparent lack of attractive π–π interactions that are often observed in this type of system.[14] There is neither face-to-face dimerization of porphinato moieties as observed in [Fe(OEP)(OClO$_3$)]$_2$ nor π-interaction from the solvent molecule as observed in Fe(TPP)(OClO$_3$)·0.5xyl. Consequently, an important feature of the crystal structure of Fe(TPP)(OReO$_3$)·tol is the fact that the iron atom is not even weakly coordinated to a "sixth ligand", as in several other ostensibly five-coordinate iron(III) porphyrin species.[14]

Face-to-face π-interaction, in which pyrrole rings on opposing metalloporphyrins are attracted to one another, is characterized by a short mean plane separation and significant overlap of the two macrocycles.[14] Both criteria are absent in Fe(TPP)(OReO$_3$)·tol. First, the perpendicular distance between the mean planes of TPP groups is 4.55 Å, compared to 3.51 Å for [Fe(OEP)(OClO$_3$)]$_2$. Second, there is little overlap of ring systems (see Figure 4b). The lateral slip[14] serves as a measure of the amount of overlap and is 6.66 Å in Fe(TPP)(OReO$_3$) but only 3.42 Å in [Fe(OEP)(OClO$_3$)]$_2$.

Several metal tetraphenylporphyrin complexes display π-complexes with small aromatic molecules where the solvate and porphyrin planes are almost parallel. Scheidt and Lee note that, in these cases, "the metal atom is always an apparent point of the π interaction" and "an electron-rich carbon of the aromatic solvent

(21) Barkigia, K. M.; Fajer, J.; Alder, A. D.; Williams, G. J. B. *Inorg. Chem.* **1980**, *19*, 2057.

Table IV. Important Parameters for Five-Coordinate Iron(III) Porphyrin Compounds

compd	ΔFe–N_4, Å	ΔFe–core, Å	Fe–O(L), Å	Ct′–N, Å	av Fe–N, Å	magnetic moment,[a] μ_B	δ, mm/s	ΔE_Q, mm/s	$\%S = {}^3/_2$	ref
Fe(TPP)$B_{11}CH_{12}$	0.13	0.10		1.955	1.961	4.2	0.33	4.12	92	23
Fe(OEP)($OClO_3$)	0.26	0.26	2.067	1.977	1.994	4.7	0.37	3.57	82	2
Fe(TPP)($OClO_3$)	0.28	0.30	2.029	1.981	2.001	5.2	0.38	3.5	65	1
Fe(TPP)($OReO_3$)	**0.44**	**0.48**	**2.024**	**2.011**	**2.059**	**5.5**	**0.43**	**1.32**	**20 ± 10**	**this work**
Fe(TTP)OAc[b]	0.485	0.52	1.898	2.010	2.067	5.9	not reported	not reported	0	4
Fe(TPP)F	0.47	0.47		2.018	2.072	5.9	not reported	not reported	0	28

[a] Room temperature. [b] (Acetato)(5,10,15,20-tetra-*p*-tolylporphyrinato)iron(III).

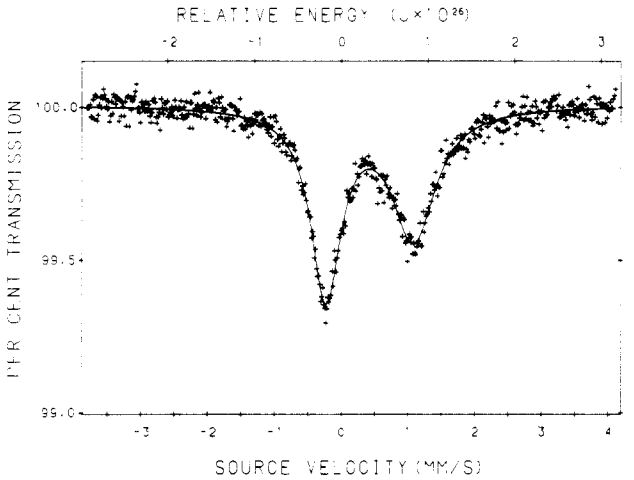

Figure 5. Mössbauer spectrum of Fe(TPP)($OReO_3$)·tol obtained at 78 K.

is always close to the metal atom".[14] But in the case of Fe(TPP)($OReO_3$)·tol, the angle between the porphyrin and toluene planes is 43°, as compared to less than 12° in other systems.[14] The C(S4) para carbon atom of the toluene molecule is closest to the iron atom at 4.17 Å. However, the closest intermolecular contacts of the toluene molecule are between perrhenate oxygen atoms and a toluene ortho carbon atom: O(4)–C(S6) 3.38 (2) Å and O(2)–C(S6) = 3.45 (3) Å.

Mössbauer Spectroscopy. The Mössbauer spectrum of Fe(TPP)($OReO_3$)·tol, obtained at 78 K, is shown in Figure 5. The hyperfine parameters of the quadrupole doublet are 0.43 mm/s for the isomer shift and 1.32 mm/s for the quadrupole splitting. The doublet has equal-area component lines whose widths are 0.55 mm/s for the low-velocity component and 0.80 mm/s for the high-velocity component. The observed percent absorption and the absolute absorption area of 1.02 (% effect) (mm/s) are small because of the fact that the absorber contained only 19 mg/cm^2 of materials, as compared to the ideal absorber thickness of 59 mg/cm^2, and because of the presence of rhenium, which has a mass absorption coefficient of 160 cm^2/g at 14.4 keV. In this study the absorber thickness was reduced because of the limited sample available. The observed hyperfine parameters are typical of iron(III) porphyrin complexes that are predominantly high-spin in character.[1,22,23] However, the very different line widths observed for the two components of the quadrupole doublet are very characteristic of electronic spin state relaxation[24] on the Mössbauer time scale of 10^{-8} s and may indicate the presence of some relaxation between the $S = {}^3/_2$ and $S = {}^5/_2$ spin states even at 78 K.

Iron Spin State. As mentioned in the introduction both high-spin and intermediate-spin states have been observed in Fe^{III}(porphyrin)X systems. For Fe(TPP)X compounds the room-temperature magnetic moments have varied from 4.0 to 5.9 μ_B.[25] Intermediate-spin magnetic moment values in these compounds are found in systems where the axial ligand X^- provides a very weak field and poor coordinating ability. These have been explained as arising from various quantum admixtures of $S = {}^3/_2$ and $S = {}^5/_2$ states.[1] The amount of $S = {}^3/_2$ state in Fe(TPP)X systems has been found to vary from 98% in Fe(TPP)($FSbF_5$)·C_6H_5F ($\mu = 4.05\ \mu_B$)[26] to 65% in Fe(TPP)($OClO_3$)·0.5xyl ($\mu = 5.2\ \mu_B$).[1]

Where does $OReO_3^-$ fit in the spectrochemical series? Although there is but a limited amount of work with $OReO_3^-$ as a ligand, Lenz and Murmann have investigated the $[Co(NH_3)_5X](NO_3)_3$ system, where X^- is $OReO_3^-$, Cl^-, and $OClO_3^-$.[16] Their results, based on visible spectral measurements, showed that $OReO_3^-$ was near Cl^- in the spectrochemical series. They also found that $OReO_3^-$ and Cl^- were coordinated as X^- ligands in the $[Co(NH_3)_5X](NO_3)_3$ system but $OClO_3^-$ was not coordinated. In this study, we have found that although $OClO_3^-$ and $OReO_3^-$ both coordinate to iron to form Fe(TPP)X, water (in the form of water of hydration) readily replaces the perchlorate, but not the perrhenate, from the coordination sphere in [Fe(TPP)X]·$2H_2O$.[17] Thus the order of the ligand field strengths is $Cl^- > ReO_4^- > ClO_4^-$, where Fe(TPP)($OReO_3$) could exhibit properties reflecting a quantum-mechanical admixture of $S = {}^3/_2$ and $S = {}^5/_2$ spin states with a predominant amount of the $S = {}^5/_2$ state.

A variety of data in both solid state and solution support this expectation. First, the solid-state room-temperature magnetic moment of 5.5 μ_B is lower than that expected and observed for pure high-spin forms ($\mu = 5.9\ \mu_B$) but higher than that found for both the pure intermediate $S = {}^3/_2$ spin state ($\mu = 3.9\ \mu_B$) and the Fe(TPP)($OClO_3$) system, which contains 65% $S = {}^3/_2$ ($\mu = 5.2\ \mu_B$). Second, the chemical shift of the pyrrole protons at 60.6 ppm for Fe(TPP)($OReO_3$) in $CHCl_3$, first measured by Goff[5] and repeated in this work, falls near those of pure high-spin forms (70–75 ppm) but significantly above those found in compounds with large amounts of the $S = {}^3/_2$ state, e.g., 13 ppm for Fe(TPP)($OClO_3$).[27] Third, although the Mössbauer effect hyperfine parameters are typical of the $S = {}^5/_2$ spin state, the line shape does show the presence of possible relaxation with the $S = {}^3/_2$ state. The structural parameters of these five-coordinate Fe(TPP)X systems are also consistent with the placement of perrhenate between Cl^- and $OClO_3^-$ in ligand field strength.

Reed[1] has predicted and shown that the ligand with the weakest interaction will provide the smallest amount of displacement of the iron from the porphyrin plane or four-nitrogen plane, the shortest Fe–N distance, the smallest porphyrin core hole (given by the Ct–N distance), and the longest Fe–X bond distance. Table IV compares these parameters for Fe(TPP)(ReO_3)·tol and several representative Fe(TPP)X systems. Arranging the compounds in order of the percent of $S = {}^3/_2$ shows that the perrhenate parameters lie between those for admixed spin states with primarily the $S = {}^3/_2$ state and fully high-spin states. The 0.44-Å displacement from the four-nitrogen plane of the Fe in Fe(TPP)($OReO_3$) is significantly greater than the Fe(TPP)$B_{11}CH_{12}$ (92% $S = {}^3/_2$) value of 0.13 Å[23] and near the 0.47 Å value for high-spin

(22) Long, G. J.; Cranshaw, T. E.; Longworth, G. *Mössbauer Effect Ref. Data J.* **1983**, *6*, 42.
(23) Gupta, G. P.; Lang, G.; Young, J. L.; Scheidt, W. R.; Shelly, K.; Reed, C. R. *Inorg. Chem.* **1987**, *26*, 3022.
(24) Grandjean, F. Mössbauer Spectral Lineshapes in the Presence of Electronic State Relaxation. In *The Time Domain in Surface and Structural Dynamics*; Long, G. J., Grandjean, F., Eds.; Kluwer Academic Publishers: Boston, MA, 1988; p 287.
(25) Gupta, G. P.; Lang, G.; Reed, C. A.; Shelly, K.; Scheidt, W. R. *J. Chem. Phys.* **1987**, *86*, 5288.
(26) Shelly, K.; Bartczak, T.; Scheidt, W. R.; Reed, C. A. *Inorg. Chem.* **1985**, *24*, 4325.
(27) Boersma, A. D.; Goff, H. M. *Inorg. Chem.* **1982**, *21*, 581.

Fe(TPP)F.[28] Column 5 in Table IV shows the hole sizes are essentially the same in Fe(TPP)($OReO_3$) and the high-spin acetate system. But we can note that the average Fe–N distances increase from 1.961 Å for Fe(TPP)$B_{11}CH_{12}$ to 2.059 Å for Fe(TPP)($OReO_3$) to 2.072 Å for Fe(TPP)F. Also, in the cases where there are Fe–O bonds, the distances decrease in a monotonic fashion from 2.067 Å in Fe(OEP)($OClO_3$) to 2.024 Å in Fe(TPP)($OReO_3$) to 1.898 Å in Fe(TTP)OAc.

These data place the amount of the $S = {}^3/_2$ state in the 20 ± 10% range in the admixture of $S = {}^3/_2$ and $S = {}^5/_2$ spin states for Fe(TPP)($OReO_3$)·tol, which is the smallest amount thus far reported for Fe(TPP)X intermediate-spin systems.

(28) Anzai, K.; Hatano, K.; Young, J. L.; Scheidt, W. R. *Inorg. Chem.* **1981**, *20*, 2337.

Acknowledgment. We thank Richard Austin at the University of Texas in Austin for measuring the NMR spectra and Mrs. Cynthia Day of Crystalytics Co., Lincoln, NE, for collecting the X-ray data. B.B.H. (Grant No. B-483) and G.L.P. (Grant No. R-1054) thank The Robert A. Welch Foundation for their support of this work. G.J.L. thanks the donors of the Petroleum Research Fund, administered by the American Chemical Society, for support of this research.

Registry No. Fe(TPP)($OReO_3$), 95978-32-8; Fe(TPP)($OReO_3$)·tol, 129916-89-8; Fe(TPP)Cl, 16456-81-8; $AgReO_4$, 7784-00-1.

Supplementary Material Available: Textual and tabular details of the crystal structure analysis and listings of bond distances, bond angles, anisotropic thermal parameters, and least-squares planes (14 pages); a table of observed and calculated structure factors (22 pages). Ordering information is given on any current masthead page.

Contribution from the Departments of Chemistry, Faculty of Science, Alexandria University, Alexandria, Egypt, and Northeastern University, Boston, Massachusetts 02115

Synthesis and Properties of Mixed-Valence Copper Molecules (μ-Y)$N_4Cu^{II}_2Cu^{I}_2X_4$ (N = *N,N*-Diethylnicotinamide; Y = 3,4,5,6-Tetrachlorocatecholate; X = Cl, Br, I) and the Products and Kinetics of Their Reactions with Dioxygen in Nitrobenzene

Mohamed A. El-Sayed*[,1a] and Geoffrey Davies*[,1b]

Received December 18, 1989

Tetranuclear copper(I) complexes $[NCuX]_4$ (N = *N,N*-diethylnicotinamide; X = Cl, Br, I (Ia–c, respectively)) react stoichiometrically with equimolar 3,4,5,6-tetrachloro-1,2-benzoquinone (Cl_4BQ) under dinitrogen at room temperature in methylene chloride or nitrobenzene to give tetranuclear mixed-valence copper products (μ-Y)$N_4Cu^{II}_2Cu^{I}_2X_4$ (Va–c, respectively), where Y is 3,4,5,6-tetrachlorocatecholate. The electronic spectra of Va–c contain maxima in the region 750–820 nm that are due to their copper(II) centers. The maximum molar absorptivities decrease as X is changed from Cl to Br to I and the corresponding wavelengths decrease when X is changed from Br to Cl to I. Molecules Va–c are oxidized by dioxygen in ambient nitrobenzene with stoichiometry $\Delta[VI]/[O_2] = 2.0 \pm 0.1$ to give tetranuclear mono(oxo)mono(catecholato)copper(II) complexes (μ-O,μ-Y)$[NCuX]_4$ (VIa–c, respectively). Products VI have larger maximum molar absorptivities than the respective products V in the 600–900-nm region. Absorptivity of VI is larger with X = Br than with X = Cl and smaller with X = I. The spectra of (μ-Y)$_2[NCuX]_4$ (Y = O (II), CO_3, or 3,4,5,6-tetrachlorocatecholate (IV)) with fixed X = Cl or Br are very similar. Rhombic EPR spectra with four hyperfine lines for solid mixed-valence complexes Va–c at 300 K indicate trigonal-pyramidal geometry for their copper(II) centers with no evidence for significant copper(I)–copper(II) interactions. The EPR spectra of VIa–c in methylene chloride are isotropic at 300 K and rhombic with more than four hyperfine lines at 130 K, indicating more than one kind of copper(II) site. Comparison of the solid-state EPR spectra of (μ-O)$_2[NCuCl]_4$ (IIa), IVa, Va, and VIa at 300K indicates that (a) IIa contains square-pyramidal copper(II), (b) solid IVa has different copper(II) centers despite having only one kind of bridge, and (c) the distinct copper(II) centers of VIa can be observed in the solid state. Cyclic voltammograms of Va and VIa–c at a Pt electrode in ambient methylene chloride are quasi-reversible (E^f = 0.51, 0.52, 0.61, and 0.59 V vs SCE, respectively). Complex Va is oxidized by O_2 to VIa with a third-order rate law, as found for the oxidation of copper(I) dimers $[LCuX]_2$, where L is an *N,N,N',N'*-tetraalkyl diamine. Comparison of the kinetic data indicates assembly of an activated complex containing one O_2 and two Va molecules as the rate-determining step. By contrast, the corresponding oxidations of Vb and Vc are second-order processes, like those of complexes $[NCuX]_4$, $N_3Cu_3M(NS)X_4$, and $N_3Cu_3M(NS)_2X_4$ (NS = monoanionic *S*-methyl isopropylidenehydrazinecarbodithioate). The slowest steps appear to involve electron transfer from Vb and Vc to O_2. Respective intermediates IXb and IXc are rapidly reduced by excess Vb or Vc to the corresponding oxocopper(II) products VIb and VIc.

Introduction

There is a great deal of current interest in the structural,[2,3] chemical,[3-7] and photophysical properties of polynuclear halo(amine)copper(I) complexes because they are easily constructed, phosphorescent[8,9] polymetallic systems containing a common, catalytically active metal.[2,3,5] This paper further demonstrates their usefulness for generating mixed-valence copper complexes.[10]

Our work is concerned with the products and kinetics of the aprotic oxidation of polynuclear copper(I) complexes by dioxygen (for example, eq 1),[4] their transmetalation with $M(NS)_n$ reagents

$$\underset{\text{I}}{[NCuX]_4} + O_2 \rightarrow \underset{\text{II}}{(\mu\text{-O})_2[NCuX]_4} \quad (1)$$

$$\text{I} + M(NS)_2 \rightarrow N_3Cu_3M(NS)X_4 + N + Cu(NS)(s) \quad (2)$$

$$N_3Cu_3M(NS)X_4 + O_2 + H_2O \rightarrow \underset{\text{III}}{(\mu_4\text{-O},\mu\text{-O})N_3Cu_3M(H_2O)X_4} + \tfrac{1}{2}N_2S_2 \quad (3)$$

(eq 2)[7,10] and the reactions of the transmetalated derivatives with dioxygen (eq 3).[7,10] Here, N is a monodentate pyridine ligand,

(1) (a) Alexandria University; (b) Northeastern University.
(2) Caulton, K. G.; Davies, G.; Holt, E. M. *Polyhedron Rep.*, in press.
(3) Davies, G.; El-Sayed, M. A. In *Copper Coordination Chemistry: Biochemical and Inorganic Perspectives*; Karlin, K. D., Zubieta, J., Eds.; Adenine Press: Guilderland, NY, 1983; p 281 and references therein.
(4) Davies, G.; El-Sayed, M. A. *Inorg. Chem.* **1983**, *22*, 1257.
(5) Karlin, K. D.; Gultneh, Y. *Prog. Inorg. Chem.* **1987**, *35*, 219.
(6) (a) Churchill, M. R.; Davies, G.; El-Sayed, M. A.; Fournier, J. A.; Hutchinson, J. P.; Zubieta, J. A. *Inorg. Chem.* **1984**, *23*, 783. (b) El-Sayed, M. A.; El-Toukhy, A.; Davies, G. *Inorg. Chem.* **1985**, *24*, 3387.
(7) Davies, G.; El-Sayed, M. A.; El-Toukhy, A.; Gilbert, T. R.; Nabih, K. *Inorg. Chem.* **1986**, *25*, 1929.
(8) Vogler, A.; Kunkely, H. *J. Am. Chem. Soc.* **1986**, *108*, 7211. Hardt, H. D.; Pierre, A. *Inorg. Chim. Acta* **1977**, *25*, L59. Hardt, H. D.; Pierre, A. Z. *Anorg. Allg. Chem.* **1973**, *407*, 107. De Ahna, H. D.; Hardt, H. D. *Z. Anorg. Allg. Chem.* **1972**, *387*, 61.
(9) Henary, M.; Zink, J. I. *J. Am. Chem. Soc.* **1989**, *111*, 7407.
(10) (a) Davies, G.; El-Sayed, M. A.; El-Toukhy, A.; Henary, M.; Gilbert, T. R. *Inorg. Chem.* **1986**, *25*, 2373. (b) Davies, G.; El-Sayed, M. A.; El-Toukhy, A.; Henary, M.; Kasem, T. S.; Martin, C. A. *Inorg. Chem.* **1986**, *25*, 3904.

0020-1669/90/1329-4891$02.50/0